Systems & Control Transactions

Research Article - Peer Reviewed Conference Proceeding
ESCAPE 35 - European Symposium on Computer Aided Process Engineering
Ghent, Belgium. 6-9 July 2025
Jan F.M. Van Impe, Grégoire Léonard, Satyajeet S. Bhonsale,
Monika E. Polańska, Filip Logist (Eds.)

PSE PRESS

High-pressure Membrane Reactor for Ammonia Decomposition: Modeling, Simulation and Scale-up using a Python-Aspen Custom Modeler Interface.

Leonardo A. C. Avilez, Antonio E. Bresciani, Claudio A. O. Nascimento, and Rita M. B. Alves*

Universidade de São Paulo, Escola Politécnica, Departament of Chemical Engineering, São Paulo, SP, Brazil.
* Corresponding Author: rmbalves@usp.br

ABSTRACT

One of the current challenges for hydrogen-related technologies is its storage and transportation. The low volumetric density and low boiling point require high-pressure and low-temperature conditions for effective transport and storage. A potential solution to these challenges involves storing hydrogen in chemical compounds that can be easily transported and stored, with hydrogen being released through decomposition processes. Ammonia stands out as a promising hydrogen carrier due to its high hydrogen content (17.8% by weight), relatively mild liquefaction conditions (~10 bar at 25°C), and the availability of a well-established storage and transportation infrastructure. The objective of this study was to develop a mathematical model to analyze and design a membrane fixed-bed reactor (MFBR) for large-scale ammonia decomposition. The kinetic model for the Ru-K/CaO catalyst was obtained from the literature and validated using the experimental data reported in the original study. This catalyst was selected due to its effective performance under high-pressure conditions, which increases the drive force for hydrogen permeation in the membrane reactor. The model was developed in Aspen Custom Modeler (ACM) using a 1D pseudo-homogeneous approach. The governing equations for mass, energy, and momentum conservation were discretized via a first-order backward finite difference method. The effectiveness factor was incorporated to account for intraparticle mass transfer limitations, which are prevalent with the large particle sizes typically employed in industrial applications. The study further investigated the influence of sweep gas ratio, temperature, relative pressure, and space velocity on ammonia conversion and hydrogen recovery, employing response surface methodology generated through an ACM-Python interface. The proposed multi-tubular membrane reactor achieved approximately 94% ammonia conversion and 90% hydrogen recovery, operating at an inlet temperature of 380°C and a pressure of 40 bar. Under comparable conditions of temperature, pressure, and WHSV, the membrane reactor demonstrated an approximately 41.7% higher ammonia conversion compared to a conventional fixed-bed reactor. Furthermore, the developed model is easily transferable to Aspen Plus, facilitating subsequent process conceptual design and economic analyses.

Keywords: Hydrogen, Ammonia decomposition, Membrane reactor, Reactor design, Modeling and simulation

INTRODUCTION

Hydrogen (H_2) is a key player in the transition to renewable energy sources due to its high energy density and CO_2-emission-free combustion [1]. However, hydrogen volumetric density is low compared to other conventional fuels such as gasoline, ethanol and natural gas [2]. Consequently, its storage and transportation present challenges, requiring energy-intensive methods like high-pressure compression and cryogenic liquefaction.

Currently, hydrogen is most stored as a compressed gas at 150-700 bar [3]. Another approach is liquid-phase storage, which offers a higher energy density but requires extremely low temperatures (-253°C at 1 bar)[4]. A novel potential solution involves storing hydrogen in chemical compounds that can be easily transported and

stored. Ammonia is a promising hydrogen carrier due to its high hydrogen content (17.8% by weight) and its moderate liquefaction conditions (~10 bar, 25°C), reducing transportation and storage [5].

For the strategy of using ammonia as a hydrogen carrier to be feasible, it is essential to study the decomposition process and develop more efficient reaction systems. Membrane fixed-bed reactors (MFBRs) offer advantages over conventional fixed-bed reactors, such as enabling operation at lower temperatures by selectively removing hydrogen, driving higher ammonia conversion, and reducing the costs associated with hydrogen purification. This study aimed to develop a mathematical model to analyze and design an MFBR for large-scale ammonia decomposition, using a Python-Aspen Custom Modeler (ACM) framework.

METHODS AND MODELING

A simplified schematic of the reactor is presented in Figure 1. The multi-tubular membrane fixed-bed reactor proposed in this study is based on conventional steam methane reformer (SMR) furnaces.

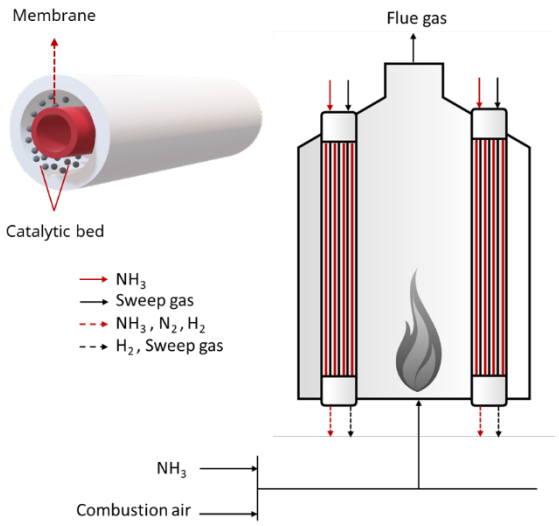

Figure 1. Simplified scheme of the multi-tubular membrane reactor.

The reaction system consists of two concentric tubes: an outer tube and an inner tube with a selective palladium membrane. The annular space between these tubes is filled with a Ru-based catalyst, where hydrogen is produced. This hydrogen permeates through the Pd membrane into the inner tube, allowing for selective separation from the reaction mixture. A sweep gas is fed into the inner tube to reduce the partial pressure of permeated hydrogen, enhancing the driving force for separation. The heat is provided to the reaction by flame using the combustion of ammonia itself, a COx-free process.

Mathematical modeling

The membrane fixed-bed reactor model was developed using a pseudohomogeneous, one-dimensional approach in Aspen Custom Modeler v.12. The main hypotheses of the model are:

1. Steady-state condition;
2. Plug-flow both in reaction and permeation zone due to the high ratio of length to diameter;
3. Negligible axial dispersion due to high calculated Peclet number;
4. Negligible pressure drop in permeation tube;
5. Constant porosity;
6. Membrane 100% selective for hydrogen.

The mass balance for each component in the annular catalytic region is described by Equation 1, while Equation 2 presents the material balance for each component in the permeation tube [6].

$$\frac{dF_{i,a}}{dz} = \eta\, r_i\, \rho_b \pi (R_2{}^2 - R_1{}^2) - 2\pi\, R_1\, J_i \quad (1)$$

$$\frac{dF_{i,t}}{dz} = 2\pi\, R_1\, J_i \quad (2)$$

where $F_{i,a}$ is the component molar flow in the annular region, η is the effectiveness factor, r_i is the component reaction rate, ρ_b is the bulk density, R_2 is outer tube radius, R_1 is the inner tube radius, $F_{i,t}$ is the component molar flow in the permeation region, and J_i is the component permeation flux through the membrane.

The kinetic model for the Ru-K/CaO catalyst, along with its parameters, was obtained from Sayas et al. [7]. The H_2 permeation flux was calculated based on Sievert's law, utilizing parameters estimated for a Pd-Ag membrane [8]. The corresponding equations for the reaction rate and H_2 permeation flux are presented in the equations 3 and 4.

$$r_{NH_3} = k\, P_{NH_3}{}^a\, P_{H_{2,a}}{}^b \left(1 - \frac{1}{K_{eq}}\left(\frac{P_{N_2}\, P_{H_{2,a}}{}^3}{P_{NH_3}{}^2}\right)\right) \quad (3)$$

$$J_{H_2} = \frac{B_H}{\delta}\left(P_{H_{2,a}}{}^{1/2} - P_{H_{2,t}}{}^{1/2}\right) \quad (4)$$

where r_{NH_3} is the ammonia consumption rate, k is rate constant, P_{NH_3} is the ammonia partial pressure, $P_{H_{2,a}}$ and $P_{H_{2,t}}$ represent the hydrogen partial pressures on the annular and permeate sides, respectively, P_{N_2} is the nitrogen partial pressure, K_{eq} is the thermodynamic equilibrium constant, J_{H_2} is the hydrogen permeation flux, B_H is the permeability, and δ is the membrane thickness.

For the effectiveness factor calculation, the kinetic

model was mathematically transformed into a pseudo-first-order kinetics, following the Pacheco et al. [9] framework. This transformation allows the Thiele modulus and the effectiveness factor to be calculated analytically.

Equations 5 and 6 present the energy balances for annular region and permeation tube [6]. It was considered that the membrane surface in contact with the reaction zone has the same temperature as the reaction itself. This assumption is reasonable because the metallic components of the membrane structure have high thermal conductivity, making their thermal resistance negligible [6].

$$\left(\sum_{i=1}^{3} F_{i,a}\, c_{p,i}\right)\frac{dT}{dz} = 2\pi\,[R_2(U_1(T_w - T)) - R_1(U_2(T - T_p))] + \pi\,(R_2{}^2 - R_1{}^2)\,\rho_b\,\eta\,r_{rxn}(-\Delta H_{rxn}) \quad (5)$$

$$\left(\sum_{i=1}^{2} F_{i,p}\, c_{p,i}\right)\frac{dT_p}{dz} = 2\pi\; R_1[U_2(T - T_p) - J_{H_2}[h_{H_2}(T_p) - h_{H_2}(T)]] \quad (6)$$

where $c_{p,i}$ is the component molar specific heat, T is the temperature in the reaction region, T_p is the temperature in the permeation region, T_w is the wall temperature, U_1 is the overall heat transfer coefficient between the reactor's outer wall and the annular reaction zone, U_2 is the overall heat transfer coefficient between the reaction and permeation zones, r_{rxn} is the ammonia decomposition rate, and h_{H_2} is the specific enthalpy of hydrogen.

The overall heat transfer coefficient between reaction tube outer wall and reaction mixture (U_1) is calculated using Dixon correlation [10], whereas the overall heat transfer coefficient between the annular region and the permeation (U_2) is considered fixed with the value of 8.64 kJ/m²·h·K [11].

For the annular catalytic region, the pressure drop along the reactor's length is calculated using the Ergun equation, as shown in Equation 7.

$$-\frac{dp}{dz} = 150\,\frac{(1-\varepsilon)^2}{\varepsilon^3}\,\frac{\mu\,u}{{d_p}^2} + 1.75\,\frac{1-\varepsilon}{\varepsilon^3}\,\frac{u^2\rho_f}{d_p} \quad (7)$$

where p is the pressure of the annular reaction zone, μ is the mixture viscosity, u is the fluid superficial velocity, d_p is the spherical equivalent particle diameter, ε is the bed porosity, and ρ_f is the fluid density.

Physical properties, including mixture density, dynamic viscosity, molar specific heat, and hydrogen specific enthalpy, were calculated using internal procedures within ACM, based on the PR-BM thermodynamic property package. This package employs the Peng-Robinson equation of state with Boston-Mathias modifications to determine the main thermodynamic properties.

The governing equations for mass, energy, and momentum conservation were discretized via first-order backward finite difference method and solved using a nonlinear equation solver. The reactor parameters are detailed in Table 1.

Table 1: Parameter setting of the ammonia cracking membrane reactor.

Parameter	Value	Reference
Tube length (m)	12	[12]
Reactor internal diameter (m)	0.1016	[13]
Membrane diameter (m)	0.0508	Adopted
Membrane thickness (μm)	7.5	[8]
Catalyst particle diameter (mm)	10	[14]
Bed voidage (Estimated)	0.404	[15]

Sensitivity analysis: Python-ACM interface

ACM enables an automated interface with Python via the comtypes module, facilitating model analysis and response surface generation. Python controls model variables and parameters, sending commands to ACM to perform simulations and record responses. The output data are processed in Python, allowing for the generation of response surfaces and detailed sensitivity analysis.

First, an isothermal reactor was considered and the effect of temperature, space velocity, permeation tube pressure and sweep gas ratio in the ammonia conversion and hydrogen recovery. After establishing the operational conditions, the rigorous model of a non-isothermal reactor was then simulated.

RESULTS

This section presents the isothermal reactor analysis to evaluate operational variables and define preliminary conditions, followed by the results for the non-isothermal model.

Effect of pressure and temperature

Figure 2 shows the effect of the tube and reaction pressures on ammonia conversion at temperatures of 350°C, 400°C, and 450°C. The results demonstrate that increasing temperature enhances ammonia conversion, consistent with the endothermic nature of the reaction. At 450°C, near-complete conversion is achieved under favorable pressure conditions (low tube pressure and high reaction pressure).

Higher reaction pressures reduce ammonia conversion due to thermodynamic limitation; however, they also enhance the driving force for hydrogen permeation through the membrane, partially compensating for this limitation. Conversely, higher tube pressures reduce the driving force for hydrogen removal, which can lower conversion efficiency. Nonetheless, they provide the ad-

vantage of delivering pressurized hydrogen, thereby reducing recompression costs.

Another important metric to evaluate is hydrogen recovery (HR), defined as the ratio of the amount of hydrogen separated through the membrane to the total amount of hydrogen produced in the reaction. Figure 3 shows the effect of tube and reaction pressures on HR at temperatures of 350°C, 400°C, and 450°C.

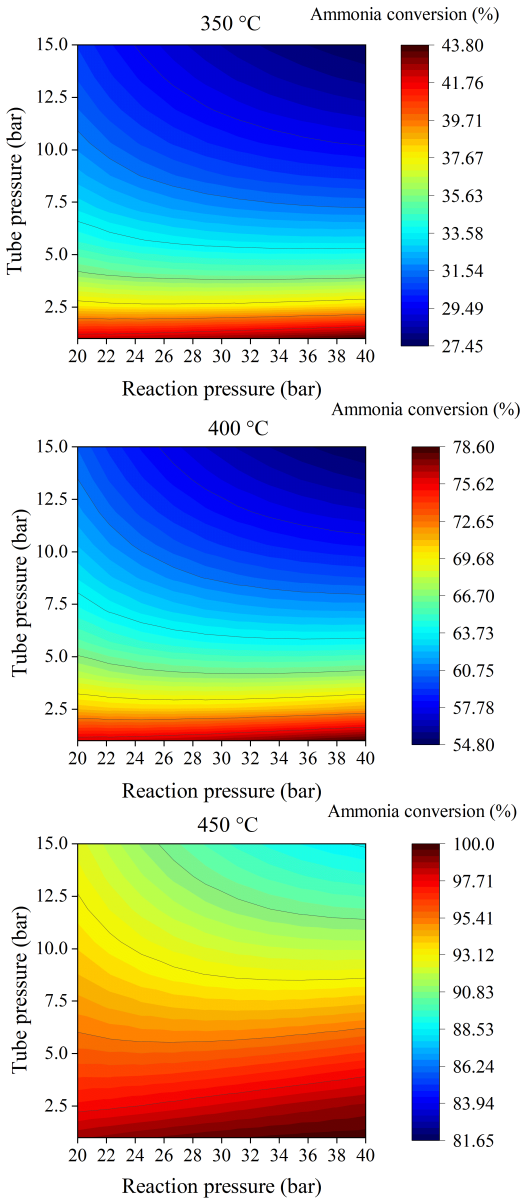

Figure 2. Effect of tube and reaction pressure at temperatures of 350°C, 400°C, and 450 °C on ammonia conversion (WHSV = 1000 g/L·h , sweep gas ratio = 0.25).

As expected, HR is enhanced by increasing the pressure difference between the reaction zone and the tube, which acts as the driving force for hydrogen permeation. Temperature also positively influences HR, as it increases the permeation rate of hydrogen. At a pressure difference of 30 bar and a temperature of 350 °C, HR is approximately 56.9%. In contrast, at 450 °C under the same pressure conditions, HR increases significantly, reaching 73.4%.

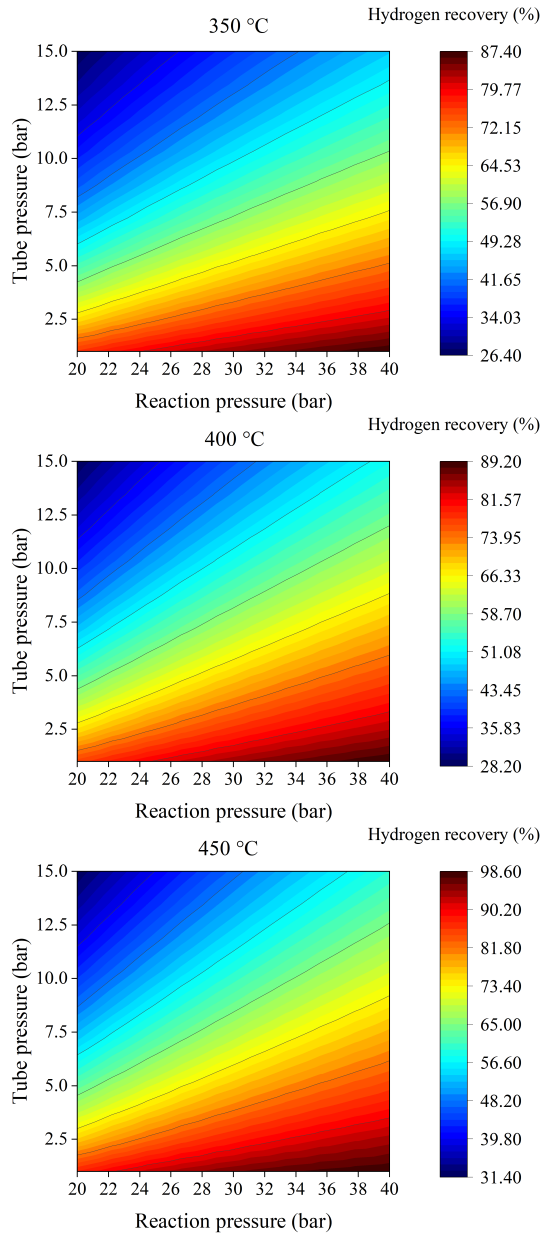

Figure 3. Effect of tube and reaction pressure at temperatures of 350°C, 400°C, and 450 °C on hydrogen recovery (WHSV = 1000 g/L·h , sweep gas ratio = 0.25).

Effect of space velocity and sweep gas ratio

Figure 4 presents the effect of WHSV (weight hourly space velocity) and sweep gas ratio (SGR) on ammonia conversion for 400 and 450°C, while also comparing the performance of the membrane fixed-bed reactor design

(MFBR) with a conventional fixed-bed reactor. The SGR, defined as the molar ratio of sweep gas to feed ammonia, influences the driving force for hydrogen permeation by reducing the partial pressure of hydrogen on the permeation side of the membrane.

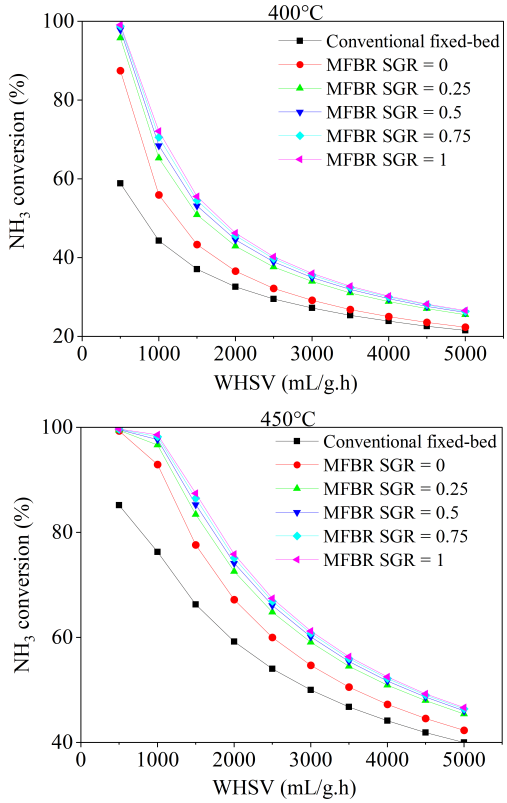

Figure 4. Effect of WHSV and sweep gas ratio (SGR) at temperatures of 400 and 450 °C on ammonia conversion (tube pressure = 5 bar, reaction zone pressure = 40 bar).

The results presented in Figure 4 indicated that the conversion gain of MFBR compared to the conventional fixed-bed reactor is more pronounced at lower WHSV values. For instance, at a WHSV of 500 mL/g·h, 400°C, and SGR of 0.25, the conversion increase is approximately 63%. In contrast, at a WHSV of 1500 mL/g·h under the same conditions, the conversion gain drops to 37%. When the temperature increases from 400 to 450 °C, overall ammonia conversion improves for both reactors due to enhanced reaction kinetics. However, at low WHSV values, the relative conversion gain of the MFBR compared to the conventional reactor reduces at 450 °C.

Additionally, increasing the SGR from 0 to 0.25 leads to considerable improvement in ammonia conversion. However, further increases in SGR beyond 0.25 yield only slight gains in conversion.

Complete model and reactor design

A reactor configuration was proposed based on the analysis of key operating variables. To better represent industrial performance, the model was extended to include non-isothermal behavior and intraparticle mass resistance. Table 2 summarizes the selected operating conditions for the complete model and reactor design.

Table 2: Operating conditions for the MFBR Simulation.

MFBR operating conditions	Value
Inlet reactor temperature (°C)	380
Sweep gas ratio	0.25
Reaction and tube pressures (bar)	40/5
WHSV (mL/g·h)	500

Figure 5 compares ammonia conversion and reaction zone temperature profiles along the reactor length for MFBR and conventional fixed-bed reactors under the same operating conditions.

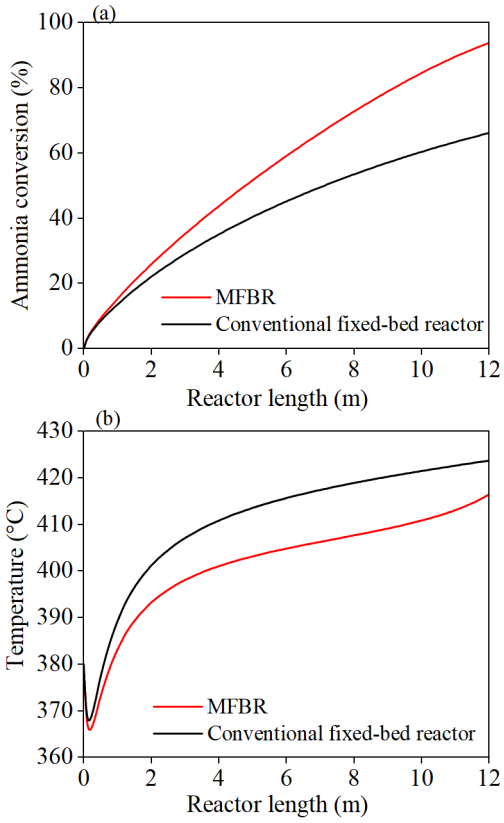

Figure 5. Profiles of ammonia conversion (a) and reaction zone temperature (b) along the reactor length for MFBR and conventional fixed-bed reactors (T_w = 430 °C).

The proposed MFBR demonstrated an approximately 41.7% higher ammonia conversion compared to a conventional fixed-bed reactor. The conversion profile indicates that the reaction occurs along the entire reactor

length, ensuring effective utilization of the reactor volume without underutilized sections.

Regarding the temperature profile, an initial drop is observed in both reactors. This behavior can be explained by the reaction's endothermic nature, where a higher reaction rate near the reactor inlet, driven by the elevated partial pressure of ammonia, results in significant heat consumption. Despite the same fixed wall temperature for both reactors, the MFBR exhibits a lower temperature profile along the reactor length due to its higher ammonia conversion.

Considering a large-scale ammonia decomposition unit with the production of 200 tons per day of hydrogen, the proposed reactor would require 1017 tubes.

CONCLUSION

A unidimensional pseudohomogeneous model describing a multi-tubular membrane reactor for ammonia decomposition was developed. The proposed reactor configuration achieves 94% ammonia conversion and 90% hydrogen recovery, representing a 41.7% higher conversion compared to the traditional reactor. These results are promising and provide a foundation for scaling up the ammonia decomposition process in membrane reactors.

Overall, the MFBR offers several advantages compared to the traditional fixed-bed reactor. It enables operation at lower temperatures due to its higher conversion rates and avoids the need for costly hydrogen separation steps, resulting in potential environmental and economic benefits. In future work, a more detailed 2D model incorporating radial dispersion effects will be developed and the results of both models will be compared.

ACKNOWLEDGEMENTS

The authors gratefully acknowledge the support of the São Paulo Research Foundation (FAPESP) (#2022/15230-5, #2024/08858-9) and Petronas for the financial support and ANP (Brazilian National Oil, Natural Gas, and Biofuels Agency) for the strategic importance of its support through the R&D levy regulation.

REFERENCES

1. Huang X, Lei K, Mi Y, Fang W, Li X. Recent progress on hydrogen production from ammonia decomposition: technical roadmap and catalytic mechanism. *Molecules* 28:5245 (2023).
2. Lee JE, Lee J, Jeong H, Park Y-K, Kim B-S. C. Catalytic ammonia decomposition to produce hydrogen: A mini-review. *Chem Eng J* 475:146108 (2023).
3. Hjeij D, Biçer Y, Koç M. Hydrogen strategy as an energy transition and economic transformation avenue for natural gas exporting countries: Qatar as a case study. *Int J Hydrogen Energy* 47:4977-5009 (2022).
4. Züttel A. Hydrogen storage methods. *Naturwissenschaften* 91:157-172 (2004).
5. Spatolisano E, Restelli F, Pellegrini LA, Cattaneo S, De Angelis AR, Lainati A, Roccaro E. Liquefied hydrogen, ammonia and liquid organic hydrogen carriers for harbour-to-harbour hydrogen transport: A sensitivity study. *Int J Hydrogen Energy* 32: 1424-1431 (2024).
6. De Falco M, Dipaola L, Marrelli L. Heat transfer and hydrogen permeability in modelling industrial membrane reactors for methane steam reforming. *Int J Hydrogen Energy* 32: 2902–2913 (2007).
7. Sayas S, Morlanés N, Katikaneni SP, Harale A, Solami B, Gascon J. High pressure ammonia decomposition on Ru–K/CaO catalyst. *Catal Sci Technol* 10:5027–5035 (2020).
8. Basile A, Paturzo L, Vazzana A. Membrane reactor for the production of hydrogen and higher hydrocarbons from methane over Ru/Al_2O_3 catalyst. *Chem Eng J* 93:31-39 (2003).
9. Pacheco M, Sira J, Kopasz J. Reaction kinetics and reactor modeling for fuel processing of liquid hydrocarbons to produce hydrogen: isooctane reforming. *Appl Catal A Gen* 250:161-175 (2003).
10. Dixon AG. An improved equation for the overall heat transfer coefficient in packed beds. *Chem Eng Process* 35:323-321 (1996).
11. Madia GS, Barbieri G, Drioli E. Theoretical and experimental analysis of methane steam reforming in a membrane reactor. *Can J Chem Eng* 77:698-706 (1999).
12. Caballero JJB, Zaini IN, Yang W. Reforming processes for syngas production: A mini-review on the current status, challenges, and prospects for biomass conversion to fuels. *Appl Energy Combust Sci* 10:100064 (2022).
13. Li P, Chen L, Xia S, Kong R, Ge Y. Multi-objective optimal configurations of a membrane reactor for steam methane reforming. *Energy Reports* 8:527-538 (2022).
14. Pedernera MN, Piña J, Borio DO, Bucalá V. Use of a heterogeneous two-dimensional model to improve the primary steam reformer performance. *Chem Eng J* 94:29-40 (2003).
15. Benyahia F, O'Neill KE. Enhanced Voidage Correlations for Packed Beds of Various Particle Shapes and Sizes. *Particulate Science and*

Technology 23:169-177 (2005).